PCCP

PAPER

View Article Online
View Journal | View Issue

Cite this: *Phys. Chem. Chem. Phys.*, 2016, **18**, 30047

Received 13th September 2016,
Accepted 12th October 2016

DOI: 10.1039/c6cp06314d

www.rsc.org/pccp

Nitrosodisulfide $[S_2NO]^-$ (perthionitrite) is a true intermediate during the "cross-talk" of nitrosyl and sulfide†

Juan P. Marcolongo,* Uriel N. Morzan, Ari Zeida, Damián A. Scherlis and José A. Olabe*

Nitrosodisulfide S_2NO^- is a controversial intermediate in the reactions of *S*-nitrosothiols with HS^- that produce NO and HNO. QM-MM molecular dynamics simulations combined with TD-DFT analysis contribute to a clear identification of S_2NO^- in water, acetone and acetonitrile, accounting for the UV-Vis signatures and broadening the mechanistic picture of N/S signaling in biochemistry.

I. Introduction

In addition to the diverse biological roles of nitric oxide NO,[1] subsequent developments have attracted attention to another "gasotransmitter", H_2S.[2,3] Both species are endogenously produced in humans and show multiple actions relevant to animal physiology (regulation of blood pressure, neurotransmission, immune response, *etc.*) as well as to plant physiology (regulation of plant defense responses, stomatal closure, abiotic stress, seed germination, *etc.*).[4–7] The NO signaling cascade has been increasingly well characterized through the identification and chemical properties of distinct nitrosyl redox-states (NO^+, $NO^\bullet$, NO^-/HNO).[7–9] On the other hand, the biological-pharmacological effects of sulfides are less understood, and species other than H_2S could be responsible for signaling. This is the case for sulfane sulfur, S^o, an uncharged form of sulfur with six valence electrons having a unique ability to attach reversibly to other sulfur atoms such as elemental sulfur (S_8), persulfides (RSSH), polysulfides (HS_n^-, n = 2–7), thiosulfate ($S_2O_3^{2-}$), and others.[10–14]

More recent is the growing appreciation that both gases often exert similar and, in part, interdependent biological actions within the same model system resulting in either mutual attenuation or potentiation responses, the so-called NO/H_2S "cross-talk".[15–22] New biological mediators might be involved, and attention is being directed to some early-described N–S hybrid species such as thionitrous acid (which we describe generically as HSNO, though other isomers HONS and SN(H)O might exist in rapid tautomeric equilibria at pH 7.4),[23] thionitrite (SNO^-) and perthionitrite (S_2NO^-),[24] the sulfur analog of peroxynitrite (O_2NO^-).

S-Nitrosation of thiols is an important NO-signaling process for protein modifications; actually, the mechanisms involved are a matter of significant debate. *S*-Nitrosothiols, RSNOs, may be formed with some degree of specificity on particular protein thiols. The currently discussed routes for their degradation and redistribution are not sufficient to explain the vast array of specific and targeted responses of NO that have been attributed to *S*-nitrosation.[25] In a general way, *S*-nitrosothiols may interchange the NO-attached thiolate groups through the so-called transnitrosation reaction (1):

$$RSNO + R'S'H \rightleftarrows R'S'NO + RSH \qquad (1)$$

The reactions of H_2S with low-molecular weight and/or protein RSNOs might afford a new scenario for the modulation of the RSNO profile in the cells.[26] It is currently accepted that HSNO can be initially formed *via* the transnitrosation of RSNOs with H_2S. Reaction (1′) describes the specific case for nitrosoglutathione, GSNO,[26,27] for which $k_{1'} = 84\ M^{-1}\ s^{-1}$ has been reported.[26]

$$GSNO + HS^- + H^+ \rightleftarrows HSNO + GSH \qquad (1')$$

HSNO possesses a mobile and ionisable H-atom instead of the alkyl groups of other RSNOs; though it is currently considered as the "smallest" and even the "simplest" member of the RSNO family, HSNO affords a unique chemistry leading, *e.g.*, to hydrodisulfide, HS_2^-, a different reactive species as compared to alkyl disulfides, R_2S_2.[20,23]

The rich chemistry of HSNO has been under close scrutiny, given its potential ability to form a second generation of intermediates with putative specific signaling roles.[26–29] Related to

Departamento de Química Inorgánica, Analítica y Química Física and INQUIMAE-CONICET, Facultad de Ciencias Exactas y Naturales, Universidad de Buenos Aires, Ciudad Universitaria, Pab. 2, C1428EHA Buenos Aires, Argentina. E-mail: olabe@qi.fcen.uba.ar, jmarcolongo@qi.fcen.uba.ar

† Electronic supplementary information (ESI) available: Computer simulation details, field parameters of the different solvents used in the simulations, electronic spectra calculated for the species presented in Table 1 and accumulated work obtained in the free energy profile calculations. See DOI: 10.1039/c6cp06314d

reaction (1′), the mixture of reactants at pH 7.4[26] or 11[27] tracked the decay of GSNO (λ_{max}, 334 nm) with the onset of an intermediate, I_{yellow}. A clear isosbestic point at 375 nm was established with the growing UV-vis absorption band of I_{yellow}, centered at 412 nm. It attained its maximum absorbance value in minutes, and was moderately stable on the hour time scale, revealing a slow decay. The observed UV-vis display does not match however with the stoichiometry of reaction (1′), given that HSNO has been reported to absorb at 330–340 nm, not at 412 nm.[26–30] Positive evidence for HSNO has been reported with mass spectrometric (MS) cryogenic experiments,[26] and recent computations support the thermodynamic stability and interconvertibility of several HSNO isomers in aqueous media.[23] On the basis of the high reactivity expected for HSNO at room temperature, the competitive reactions (2) and (3) have been proposed, as similarly observed with RSNOs.[18]

$$HSNO \rightleftarrows NO + S^{\bullet -} + H^{+} \quad (2)$$

$$HSNO + HS^{-} \rightleftarrows HNO + HS_2^{-} \quad (3)$$

Reaction (2) implies a fast homolytic cleavage of the S–N bond (expectedly weaker in HSNO than in RSNOs), with the production of reactive $S^{\bullet -}$ radicals that lead to disulfide.[31,32] Under excess sulfide, the formation and reactivity of $HS_2^{\bullet 2-}$ radicals[31] may produce disulfides under catalytic conditions.[32] Disulfides are also direct products in reaction (3), along with HNO.

The N/S hybrid SNO^- and S_2NO^- ions have been well characterized as solid salts,[24] though their clear identification and chemistry in aqueous solutions remains elusive. Early generated yellow species with λ_{max} at ~410 nm have been observed in the studies of the reactions of HS^- with other RSNOs like *S*-nitrosocysteine (CysNO), *S*-nitrosopenicilammine (SPEN) and *S*-nitroso-*N*-acetylpenicilammine (SNAP), as well as with NO and NO-donors (NONOates).[26–29] Controversial views on the identity of I_{yellow} have been exposed, coupled to uncertainties on its generation mode and further reactivity.[26–30] We aim to contribute to the latter problem through a main computational approach that confirms the identity of S_2NO^- in water and aprotic solvents, along with a mechanistic analysis that highlights its generation mode and, in a more general context, the role of disulfides in biochemistry. Modern computational methodologies have been successfully employed recently through the modeling of charged and polar residues in proteins in order to elucidate how they could control RSNO-reactivity.[33]

II. Methodology

We perform an exhaustive theoretical investigation based on a combination of state of the art electronic structure strategies, including quantum mechanics – molecular mechanics (QM-MM) and real time TD-DFT simulations, seeking to elucidate the identity of I_{yellow}. Sections II.1, II.2 and II.3 describe the main features of the simulations.

II.1 Details of the QM-MM molecular dynamics simulations

QM-MM simulations were carried out using the LIO package, a DFT code for gaussian basis sets developed within our group[34,35] in combination with AMBER12 for the description of the classical subsystem. The protocols utilized within the present work are discussed in detail in ref. 35–37. For the QM region, computations were performed at the generalized gradient approximation (GGA) level, using the PBE exchange and correlation functional, with a dzvp basis set. The electronic density was also expanded in an auxiliary basis set and the fitting coefficients were computed by minimizing the error in the Coulomb repulsion energy.[34]

The MM subsystem was conformed by the solvent molecules. A TIP3P potential was utilized to describe the water molecules and a six-site force field was designed for acetonitrile.[38] The force fields for acetone and dichloromethane were generated following the standard procedures for this kind of calculation: partial charges were computed using the restricted electrostatic potential (RESP) technique and DFT calculations at the PBE/dzvp level (see ESI†). Equilibrium distances and angles, as well as force constants were computed using the same electronic structure scheme.

Simulations were performed under N, p, T conditions. Temperature and pressure were kept constant using a Langevin thermostat and a Berendsen barostat.

II.2 Absorption spectral calculations

The absorption spectra of all the molecules presented in this work were calculated by averaging on an ensemble of instantaneous configurations sampled through QM-MM molecular dynamics simulations of 300 ps length. Spectral line shapes were computed through the Fourier-transform of the dipole moment functions, obtained from 50 fs real-time TD-DFT calculation performed on a set of configurations extracted from the QM-MM trajectories.[35] This methodology has been proved to be reliable to predict the absorption properties of molecules and ions in solutions and in complex environments.[35,36] For a complete description of the procedure, see the ESI.†

II.3 Free energy profile

For elucidating the free energy profile of the key reaction involving disulfide/sulfide interchange, we followed a previously described procedure[37,39,40] based on the Jarzynsky equality.[41] In our case, the reaction coordinate ξ was taken as the antisymmetric combination of the distances between the nitrogen of the NO groups and the sulfur atoms of the nucleophiles HS^- and HS_2^-. The free energy curve as a function of ξ (6.75 Å long) was computed dividing the coordinate into three parts: ξ_1 (0.2 Å → 2.5 Å), ξ_2 (0.2 Å → −3 Å) and ξ_3 (−3 Å → −3.75 Å). In each coordinate, the free energy profile was determined by performing 20 independent runs moving the system at ν = 0.05 Å ps^{-1}.

III. Results and discussion

III.1 Identification of S_2NO^-

Colloidal sols (sulfur/polysulfide mixtures) may form after the onset of reactions (1′–3) at pH's ≤ 8, usually on the second-time

scale, depending on the medium, relative reactant concentrations and/or variable mixing modes that might determine a high local concentration of a given reactant.[13,26,29,30,42] They originate in the reactivity of disulfides, and have been proposed as responsible for the onset of the 412 nm band assigned to I_{yellow}.[26] The physical and chemical properties of polysulfides are not clearly understood;[11,13,42,43] besides, their most intense absorptions are reported to occur at wavelengths $\leq$300 nm in aqueous solutions.[29,36]

An alternative previous proposal[27] for identifying I_{yellow} as S_2NO^- was discarded after providing negative spectroscopic evidence (IR, ^{15}N NMR, MS).[26] This was reinforced by a claim on the intrinsic instability of S_2NO^- in water (either under acidic or neutral conditions) toward the formation of HNO and sulfur.[30] These statements are at odds with previous and recent reports: (1) the reaction between aqueous NO and NaHS or Na_2S_2 yielded transient species with λ_{max} at 409 nm,[44] assigned to S_2NO^- on the basis of the properties of the related iminium-solid salt, soluble in alcohols and aprotic solvents (λ_{max} ~425 nm and 450 nm, respectively).[24] (2) A species with λ_{max} at ~420 nm forms in seconds and survives for minutes in water/acetonitrile mixtures as well as in aqueous solutions at pH 7.4 upon dissolution of the solid salt.[30] (3) Positive electrospray ionization (ESI)-high-resolution MS (HRMS) signals derived from aqueous SNAP/HS^- mixtures at pH 7.4 have been assigned to S_2NO^-.[29] (4) S_2NO^- (generated by mixing Na_2S and GSNO at a 2 : 1 ratio in buffered solution at pH 7.4) could be handled in anaerobic medium under a controlled way, showing a slow decay of the band at 412 nm (80% absorbance remaining in 3 h). The decay-rate was enhanced in the presence of dioxygen.[45]

Fig. 1 reinforces the assignment of the species absorbing at 409–412 nm in water to S_2NO^-. Most importantly, the experimentally observed bathochromic shift of ~40 nm when going from water to the aprotic solvents is faithfully reproduced by the computational analysis. The main character of the UV-vis electronic transition is p(S) $\rightarrow$ π^*(SNO). Our calculations show

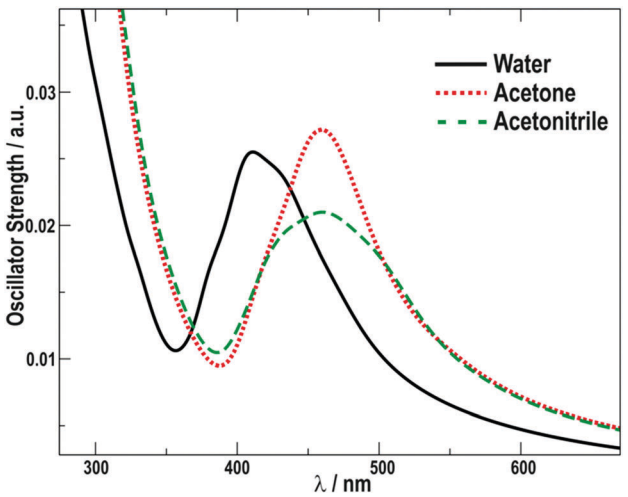

Fig. 1 Calculated spectra for S_2NO^- in water (black), acetone (red) and acetonitrile (green), using TD-DFT and QM-MM molecular dynamics simulations.

Table 1 TD-DFT calculations of N/S hybrid and related species in water and aprotic solvents. The oscillator strengths were obtained with a damping factor γ = 0.2 fs^{-1}

Compound	Solvent	λ_{max} exp/nm	λ_{max} calcd/nm (osc. str./a.u.)
$[S_2NO]^-$	H_2O	409[44]–412[28,29]	411 (0.03)
	Acetone	448[a,24,30]	458 (0.03)
	Acetonitrile	450[24]	458 (0.02)
$[O_2NO]^-$	H_2O	302[46]	307 (0.03)
	CH_2Cl_2	340[46]	339 (0.04)
EtSNO	H_2O	330[b,48]	280, 310, 330[c]
ON(SH)S	Acetonitrile	358[d,30]	368 (0.05)
HON(S)S	Acetonitrile	358[d,30]	351 (0.4)
HSNO	Water	340[e,26]	315, 360[c]
SNO^-	Acetonitrile	323[24]	315 (0.02)

[a] Also measured at 448 nm in DMSO or DMF in ref. 44. [b] Observed as a shoulder in the spectra of aqueous $[Fe^{II}(CN)_5(NOSR)]^{3-}$ ions. Also measured at 330–350 nm with free thiols in organic solvents.[48] [c] Low intensity absorption bands. [d] Assigned as a mixture of isomers ON(SH)S and HON(S)S. [e] Generated by pulse radiolysis of HS^-/NO_2^- deaerated solutions, pH 11.

that the absorption maximum for this molecule is strongly dependent on the geometrical parameters explored across the molecular dynamics. Thus, the specific interactions with the solvent become extremely important to describe the spectroscopic behavior in solution.

We have placed the computational methodology under control by performing calculations with other well characterized similar species, as detailed in Table 1, and excellent agreement with experiments has been found. Most remarkably, it can be seen that the results with O_2NO^- also account for the experimentally observed solvatochromism.[46] Solvatochromic effects have been observed for coordination compounds interacting with acceptor solvents.[47] The big UV-vis and IR spectral shifts could not be accounted for by a mere dielectric effect as produced by a continuum solvent model, and empirical donor–acceptor correlations were employed with some success, though advancing the need of using quantum-classical methodologies for a best theoretical approach. In our system, these necessities also arise both from solvent-induced structural changes and from electrostatic solute–solvent interactions, the former being dominant (see ESI†).

Table 2 shows a comparative picture of the X-ray diffraction (XRD) results[30] with data for the calculated species in solution.

A fair agreement with the reported *cis*-structure for the anion can be observed, with a trend to greater distance-values in the calculated solution spectra that can be reasonably traced to packing and environmental effects. No significant changes can be observed by comparing the geometrical features of S_2NO^- in the aprotic solvents, though subtle differences appear in water. The onset of hydrogen bonds between the negatively charged terminal sulfur S_2 ($q(S_2)$ ~ −0.7) and NO (q(NO) ~ −0.3) fragments with the solvent (see Fig. 2) determines a lower (N_1–S_1–S_2) angle in water with respect to the aprotic solvents. This accounts for the observed spectral band shift to higher energies when going to water. Interestingly, this description is also in agreement with the reported small bathochromic shift when going to alkaline solutions,[28] implying a weaker H-bonding array.

Table 2 Selected distances and angles with standard deviation for solid [PNP][S_2NO] (PNP^+ = bis(triphenyl)phosphaniminium),[30] and for the anionic species in water, acetone and acetonitrile, calculated through molecular dynamics (MD)

Parameter	XRD	MD (H_2O)	MD (acetone)	MD (acetonitrile)
$d(N_1–O_1)$/Å	1.25 (0.01)	1.24 (0.03)	1.24 (0.02)	1.24 (0.04)
$d(N_1–S_1)$/Å	1.70 (0.01)	1.79 (0.01)	1.80 (0.07)	1.80 (0.08)
$d(S_1–S_2)$/Å	1.97 (0.01)	2.07 (0.06)	2.03 (0.04)	2.04 (0.04)
$\theta(O_1–N_1–S_1)$/°	117.8 (0.2)	119 (5)	120 (4)	120 (4)
$\theta(N_1–S_1–S_2)$/°	115.1 (0.2)	111 (5)	117 (6)	117 (5)

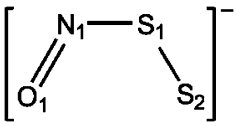

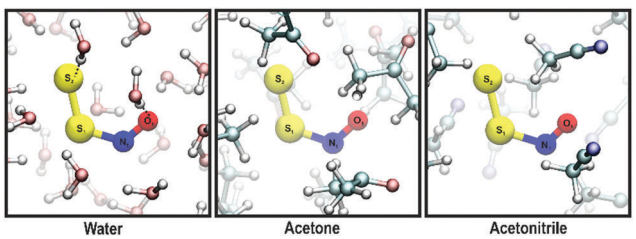

Fig. 2 S_2NO^--solvent interactions obtained by QM-MM MD simulations. Dotted lines show two selected H-bond interactions between water and S_2NO^-.

III.2 Generation mode of S_2NO^-

A third possible route for the decay of HSNO can be proposed, reaction (4), on the basis of the early generation of disulfides in the medium.

$$HSNO + HS_2^- \rightleftarrows S_2NO^- + HS^- + H^+ \qquad (4)$$

Reaction (4) is similar to a transnitrosation reaction, specifically a transnitrosopersulfidation one.[21] The interchange between the nucleophiles disulfide and sulfide at the NO-group can be described as an S^o-atom transfer. It appears as a kinetically favored reactivity mode of HSNO, compared to reaction (3). We expect a greater value for the specific rate constant k_4 than for k_3, on the basis of a greater nucleophilic ability of the more polarizable HS_2^- over HS^-. This is in agreement with predicted and observed comparative trends for persulfides and thiolates.[14,49] We confirmed these assumptions by measuring the kinetics of the disulfide addition reaction into nitroprusside, for which the specific rate-constant was found to be ~100-fold higher than for the analog reaction with sulfide.[50]

In order to validate reaction (4) by exclusively exploring the sulfide-disulfide transfer process, we performed QM-MM MD simulations in aqueous solution to determine the free energy profile for reaction (4′), which differs from (4) in the proton transfer from the weak acid HS_2NO to the medium.[51]

$$HSNO + HS_2^- \rightleftarrows HS_2NO + HS^- \qquad (4')$$

Fig. 3 shows the Jarzynski estimator for the free energy change of reaction (4′) (see ESI† for a detailed description). The reaction

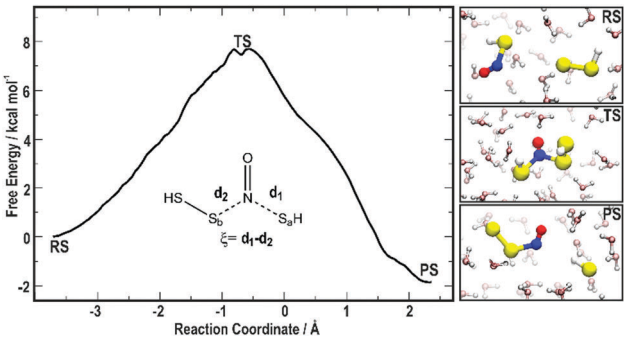

Fig. 3 Free energy profile computed for the transnitrosation reaction between HSNO and HS_2^- (4′). Right: Representative pictures of the reactant state (RS), the transition state (TS) and the product state (PS).

proceeds with $\Delta G^{\ddagger}_{4'} = 7.6\ \text{kcal mol}^{-1}$ and $\Delta G^{\circ}_{4'} = -1.9\ \text{kcal mol}^{-1}$ ($K_{4'} \sim 25$), and can be described as a fast equilibrium process. By assuming $pK_a(HS_2NO) \sim 5$, *cf.* ref. 14, K_4 can be estimated to fall in the range $\sim 10^2$–10^3 (at pH 7), consistently with the relative values of the forward/reverse specific rate constants for HS_2^-/HS^- reactivity.

The onset of reaction (4) makes the GSNO consumption through reaction (1′) autocatalytic with respect to HS_2^-. It also provides an explanation for the net GSNO → S_2NO^- conversion (334 nm → 412 nm) and the absence of specific UV-vis spectral features for HSNO. Autocatalysis is frequently associated with the build-up of induction periods for the generation of products, showing S-shaped traces.[32,36,48,52] It has been observed in the reactions of SNAP[29] and O_2NO^- (ref. 36) toward HS^-, and apparently relates to the requirement of sulfur-radicals for the generation of the more reactive HS_2^-. The induction-times increase with $[O_2]$ and decrease with $[HS^-]$,[32] and this fact relates to the observed early consumption of O_2, a trapping agent for $S^{\bullet-}$ and $HS_2^{\bullet 2-}$.[31,48] Overall, these autocatalytic features constitute nice and specific evidence supporting the proposed mechanism highlighting the role of disulfides in biochemistry.

Filipovic and coworkers considered reaction (4) only in the reverse sense, aiming to sustain a fast irreversible decomposition route for S_2NO^- upon reaction with sulfide.[30] In fact, they showed that S_2NO^- was very unstable in acidic acetone-solutions, though not in 10% water-90% acetone ones, for which the decay of the main band at ~420 nm occurred in several minutes. Moreover, the latter band also appeared by dissolving $PNP^+S_2NO^-$ under excess aqueous sulfide at pH 7.4, followed by its slow decay with $t_{1/2} \sim 7$ min. The product absorbed at 345 nm, and was assigned to HSNO by the authors. These results, instead of reflecting the "intrinsic instability" of S_2NO^- in water, certainly indicate that it reacts with HS^- although through the onset of the equilibrium reaction (4). The main band at 420 nm forms in a few seconds after dissolution and has been attributed to sulfur-sols, as evidenced by the scattering;[30] it should be best assigned to S_2NO^-, given the very small bathochromic shift compared to 408–412 nm, as demonstrated by the results in Table 1 and the trustable interpretations on the solvatochromism. The chemistry for longer time scales should be investigated further for these

complex mixtures, because reaction (4) sets up in parallel with the polysulfide/sulfur sols, and likely decomposition of the N/S hybrid compounds occurs on the minute time-scale giving NO/HNO and polysulfides.

III.3 Timing for the onset of intermediates

Once the composition and generation mode of I_{yellow} have been clearly identified, questions arise with respect to the chemistry of other intermediates NO/HNO, disulfides (eventually polysulfides and sulfur), HSNO and S_2NO^-. All of them are candidates for signaling processes. A detailed mechanistic discussion on the fate of these intermediates is over the scope of the present work, though we advance brief comments on the timing of production.

The homolytic reactivity of the N–S bond defines a main, well recognized decomposition route for nitrosothiols, comprising the reversible reaction (2).[25] The initial build-up of NO in terms of reactions (1′,2) is reinforced by a delayed formation arising in the homolytic decomposition of S_2NO^-, also giving perthiyl radicals, $S_2^{\bullet-}$. The latter process enables S_2NO^- to behave as a main carrier of substantial NO bioactivity, allowing for the activation of soluble guanylate cyclase.[29]

With respect to HNO, other generation routes could be envisaged in addition to the plausible reaction (3), namely the direct reduction of NO by HS^-,[53] or the competitive heterolytic decomposition mode for S_2NO^-.[30] Recently *N*-nitrosohydroxylamine-*N*-sulfonate, $[ONN(OH)SO_3]^-$, has been identified during the transnitrosation of RSNOs with H_2S, giving HNO upon decomposition.[29] Finally, the mechanistic details of the fate of HNO, either leading to N_2O or being further reduced to NH_2OH/NH_3, are still unknown.

Related to polysulfides, they can be currently produced through the oxidation of sulfides, or initiated through reactions (2–3). Their build-up can proceed sequentially by adding a varying number of sulfur atoms to HS^- yielding soluble sulfane chains until the number reaches 8, at which point it cyclizes and separates as colloidal elemental sulfur S_8, reaction (5).[13]

$$HS^- \rightleftarrows HS_2^- \rightleftarrows HS_3^- \rightleftarrows \cdots \rightleftarrows HS_9^- \rightarrow S_8 + HS^- \quad (5)$$

Under the underlying transnitrosation conditions, polysulfide formation seemingly arises after the exhaustive consumption of substrates in reaction (1′), as also observed with peroxynitrite reacting with HS^-.[36,54] Polysulfides are relatively stable at pHs ≥ 7, but formally disproportionate under more acidic conditions, reaction (6).[55]

$$HS_{(n+1)}^- \rightarrow n/8S_8 + HS^- \quad (n = 1\text{–}8) \quad (6)$$

Even though some disproportionation of HS_2^- is expected at pH 7.4, the "*in situ*-generation" of HS_2^- in a colloidal environment still allows a favorable competitive reactivity with other substrates, as in reaction (4).

III.4 A sulfur signaling mechanistic outlook

It is accepted that in many instances signal transductions through redox-regulated pathways occur *via* reversible oxidation of protein thiols.[21,43,56] Reactions (1–5) in this contribution constitute a set of all reversible processes, mostly appropriate for regulatory roles. Noticeably, they involve the transient generation of sulfur radicals and disulfide. Radical generation and recombination are probably related to the role of nitrosothiols in some protein modifications in the cells. Preliminary experiments showed that S_2NO^- did not cause *S*-nitrosation nor persulfidation (*S*-sulfhydration) with some model proteins, suggesting that it cannot serve as a signaling molecule.[30] The chemistry of S_2NO^- might involve S^o-transfer mechanisms (as in reaction (4)) acting in protein post-translational modifications, as reported to occur in families of *in vivo* site-specific regulatory enzymes like sulfane–sulfur transferases, some phosphatases and others.[56]

IV. Conclusions

The experimental evidence analyzed in light of the present electronic structure calculations as well as the further mechanistic considerations strongly support the early formation and survival of the S_2NO^- intermediate in the aqueous solutions, arising from the reaction between HSNO and HS_2^-. In this context, the role of both radical and/or non radical sulfur-species in signaling mechanisms remains open for further dilucidation.[56] A wide room still appears to exist for expanding the biorelevant studies dealing with HSNO and S_2NO^-.

Acknowledgements

We thank the Consejo Nacional de Investigaciones Científicas y Técnicas (CONICET) and the Universidad de Buenos Aires for financial support, and we acknowledge fruitful discussions with Dr Dario A. Estrín, Leonardo D. Slep and Sara E. Bari.

Notes and references

1 *Nitric Oxide: Biology and Pathobiology*, ed. J. L. Ignarro, Academic Press, San Diego, 2000.
2 K. Abe and H. Kimura, *J. Neurosci.*, 1996, **16**, 1066.
3 R. Wang, *Physiol. Rev.*, 2012, **92**, 791.
4 M. Yu, L. Lamattina, S. H. Spoel and G. J. Loake, *New Phytol.*, 2014, **202**, 1142.
5 Q. Li and J. R. Lancaster Jr, *Nitric Oxide*, 2013, **35**, 21.
6 M. Lisjak, T. Teklic, I. D. Wilson, M. Whiteman and J. T. Hancock, *Plant, Cell Environ.*, 2013, **36**, 1607.
7 J. M. Fukuto, C. K. Cisneros and R. L. Kincade, *J. Inorg. Biochem.*, 2013, **118**, 201.
8 S. E. Bari, J. A. Olabe and L. D. Slep, *Adv. Inorg. Chem.*, 2014, **67**, 87.
9 *The Chemistry and Biology of Azanone (HNO)*, ed. F. Doctorovich, P. J. Farmer and M. Martí, Elsevier, 2016.
10 J. I. Toohey, *Anal. Biochem.*, 2011, **413**, 1.
11 H. Kimura, *Molecules*, 2014, **19**, 16146.
12 T. V. Mishanina, M. Libiad and R. Banerjee, *Free Radicals Biol. Med.*, 2015, **11**, 457.
13 P. Nagy, *Methods Enzymol.*, 2015, **554**, 3.

14 K. Ono, T. Akaike, T. Sawa, Y. Kumagai, D. A. Wink, D. J. Tantillo, A. J. Hobbs, P. Nagy, M. Xian, J. Lin and J. M. Fukuto, *Free Radicals Biol. Med.*, 2014, **77**, 82.
15 A. Berenyiova, M. Grman, A. Mijuskovic, A. Stasko, A. Misak, P. Nagy, E. Ondriasova, S. Cacanyiova, V. Brezova, M. Feelisch and K. Ondrias, *Nitric Oxide*, 2015, **46**, 123.
16 M. L. Lo Faro, B. Fox, J. L. Whatmore, P. G. Winyard and M. Whiteman, *Nitric Oxide*, 2014, **41**, 38.
17 Q. C. Yong, J. L. Cheong, F. Hua, L. W. Deng, Y. M. Khoo, H. S. Lee, A. Perry, M. Wood, M. Whiteman and J. S. Bian, *Free Radicals Biol. Med.*, 2011, **14**, 2081.
18 S. B. King, *Free Radicals Biol. Med.*, 2013, **55**, 1.
19 Z. Miao and S. B. King, *Nitric Oxide*, 2016, **57**, 1.
20 M. M. Cortese-Krott, A. R. Butler, J. D. Woolins and M. Feelisch, *Dalton Trans.*, 2016, **45**, 5908.
21 S. E. Bari and J. A. Olabe, in *Gasotransmitters in Plants. The Rise of a New Paradigm in Cell Signalling*, ed. L. Lamattina and C. García-Mata, Springer, 2016, ch. 14, pp. 289–327.
22 G. K. Kolluru, X. Shen and C. G. Kevil, *Redox Biol.*, 2013, **1**, 313.
23 L. V. Ivanova, B. J. Anton and Q. K. Timerghazin, *Phys. Chem. Chem. Phys.*, 2014, **16**, 8476.
24 F. Seel, R. Kuhn, G. Simon, M. Wagner, B. Krebs and M. Dartmann, *Z. Naturforsch.*, 1985, **40b**, 1607.
25 K. A. Broniowska and N. Hogg, *Antioxid. Redox Signaling*, 2012, **17**, 969.
26 M. R. Filipovic, J. L. Miljkovic, T. Nauser, M. Royzen, K. Klos, T. Shubina, W. H. Koppenol, S. J. Lippard and I. Ivanović-Burmazović, *J. Am. Chem. Soc.*, 2012, **134**, 12016.
27 A. P. Munro and D. L. H. Williams, *J. Chem. Soc., Perkin 2*, 2000, **9**, 1794.
28 M. M. Cortese-Krott, B. O. Fernandez, J. L. T. Santos, E. Mergia, M. Grman, P. Nagy, M. Kelm, A. Butler and M. Feelisch, *Redox Biol.*, 2014, **2**, 234.
29 M. M. Cortese-Krott, G. G. Kuhnle, A. Dyson, B. O. Fernandez, M. Grman, J. F. DuMond, M. P. Barrow, G. McLeod, H. Nakagawa, K. Ondrias, P. Nagy, S. B. King, J. E. Saavedra, L. K. Keefer, M. Singer, M. Kelm, A. R. Butler and M. Feelisch, *Proc. Natl. Acad. Sci. U. S. A.*, 2015, **112**, 4651.
30 R. Wedmann, A. Zahl, T. E. Shubina, M. Durr, F. W. Heinemann, B. Eberhard, C. Bugenhagen, P. Burger, I. Ivanović-Burmazović and M. R. Filipovic, *Inorg. Chem.*, 2015, **54**, 9367.
31 T. N. Das, R. E. Huie, P. Neta and S. Padmaja, *J. Phys. Chem. A*, 1999, **103**, 5221.
32 K. Szacilowski, A. Wanat, A. Barbieri, E. Wasiliewska, M. Witko, G. Stochel and Z. Stasicka, *New J. Chem.*, 2002, **26**, 1495.
33 M. R. Talipov and Q. K. Timerghazin, *J. Phys. Chem. B*, 2013, **117**, 1827.
34 M. A. Nitsche, M. Ferreria, E. E. Mocskos and M. C. G. Lebrero, *J. Chem. Theory Comput.*, 2014, **10**, 959.
35 U. N. Morzan, F. F. Ramírez, M. B. Oviedo, C. G. Sánchez, D. A. Scherlis and M. C. González Lebrero, *J. Chem. Phys.*, 2014, **140**, 164105.
36 E. Cuevasanta, A. Zeida, S. Carballal, R. Wedmann, U. N. Morzan, M. Trujillo, R. Radi, D. A. Estrin, M. R. Filipovic and B. Alvarez, *Free Radical Biol. Med.*, 2015, **80**, 93.
37 A. Zeida, A. M. Reyes, M. C. González Lebrero, R. Radi, M. Trujillo and D. A. Estrin, *Chem. Commun.*, 2014, **50**, 10070.
38 X. Grabuleda, C. Jaime and P. A. Kollman, *J. Comput. Chem.*, 2000, **21**, 901.
39 M. Bringas, J. Semelak, A. Zeida and D. A. Estrin, *J. Inorg. Biochem.*, DOI: 10.1016/j.jinorgbio.2016.06.016.
40 A. Zeida, M. C. González Lebrero, R. Radi, M. Trujillo and D. A. Estrin, *Arch. Biochem. Biophys.*, 2013, **539**, 81.
41 C. Jarzynski, *Phys. Rev. Lett.*, 1997, **78**, 2690.
42 R. Wedmann, S. Bertlein, I. Macinkovic, I. S. Boltz, J. L. Miljkovic, L. E. Muñoz, M. Herrmann and M. R. Filipovic, *Nitric Oxide*, 2014, **41**, 85.
43 M. R. Filipovic, in *Chemistry, Biochemistry and Pharmacology of Hydrogen Sulfide, Handbook of Experimental Pharmacology*, ed. P. K. Moore and M. Whiteman, Springer, 2015.
44 F. Seel and M. Wagner, *Z. Anorg. Allg. Chem.*, 1988, **558**, 189.
45 C. Bolden, S. B. King and D. B. Kim-Shapiro, *Free Radicals Biol. Med.*, 2016, **99**, 418.
46 D. S. Bohle, B. Hansert, S. C. Paulson and B. D. Smith, *J. Am. Chem. Soc.*, 1994, **116**, 7423.
47 D. A. Estrín, L. M. Baraldo, L. D. Slep, B. C. Barja and J. A. Olabe, *Inorg. Chem.*, 1996, **35**, 3897.
48 K. Szacilowski and Z. Stasicka, *Prog. React. Kinet. Mech.*, 2001, **26**, 1.
49 E. Cuevasanta, M. Lange, J. Bonanata, E. L. Coitiño, G. Ferrer-Sueta, M. R. Filipovic and B. Alvarez, *J. Biol. Chem.*, 2015, **290**, 26866.
50 S. L. Quiroga, A. E. Almaraz, V. T. Amorebieta, L. L. Perissinotti and J. A. Olabe, *Chem. – Eur. J.*, 2011, **17**, 4145.
51 Reaction (4) entails a proton transfer to the solvent. Its free energy profile is difficult to compute, as it requires an averaged description of the hydronium ion in solution. The solvent should be represented quantum-mechanically, which for this system size and simulation times is computationally not affordable. Alternately, reaction (4′) does not show this drawback, and can be related to reaction 4 through the acidity of the HS_2NO species.
52 A. A. Frost and R. G. Pearson, *Kinetics and Mechanism – A Study of Homogeneous Chemical Reactions*, John Wiley & Sons, Inc., New York-London, 1961.
53 M. Eberhard, M. Dux, B. Namer, J. Miljkovic, N. Cordasic, C. Will, M. Fischer, S. A. Suarez, D. Bikiel, J. d. l. Roche, K. Dorsch, T. I. Kichko, A. Leffler, A. Babes, A. Lampert, J. K. Lennerz, J. Jacobbi, M. A. Marti, F. Doctorovich, E. D. Hoggestat, P. M. Zygmunt, I. Ivanovic-Burmazovic, K. Messlinger, P. Reeh and M. R. Filipovic, *Nat. Commun.*, 2014, **5**, 4381.
54 The reaction of O_2NO^-/O_2NOH with HS^- showed a kinetic behavior similar to the one arising with GSNO. The fast decay of the band of O_2NO^- (λ_{max}, 302 nm) led to an emergent species with λ_{max} at 408 nm, traced to a mixture of $HSNO_2$/HSONO. Intermediate HS_2^- was proposed to react with O_2NO^-/O_2NOH.
55 P. Nagy and C. Winterbourn, *Chem. Res. Toxicol.*, 2010, **23**, 1541.
56 C. C. Winterbourn, *Free Radicals Biol. Med.*, 2015, **80**, 164.

